Effect of Shielding on Radiation Detection of Weapons-Grade Plutonium

Max Eriksson
maxerikss@gmail.com

under the direction of
Dr. Débora Trombetta
Department of Physics
KTH Royal Institute of Technology

Research Academy for Young Scientists
July 14, 2021

Abstract

Nuclear material may, in the absence of regulatory control, have severe consequences. Nuclear safeguards and security are therefore of utmost importance. To improve nuclear security, the detection of nuclear material is imperative. Shielding the radioactive source will have an impact on the detectability; different shielding materials will have different results. In this study the effect of lead and polystyrene shielding on detection is tested.

A three-dimensional environment was simulated with Monte Carlo N-Particle, a particle simulation program. Among the simulations, different levels and materials of shielding were used. The simulated environment was a radiation portal monitor and the source of radiation was a cylinder of weapons-grade plutonium.

The results showed that for (γ,n), 3.0 cm lead shielded 71.61%, and 3.0 cm polystyrene shielded 61.53%; for (n,n), 3.0 cm lead shielded 14.79%, and 3.0 cm polystyrene shielded 77.91%. The drawn conclusion is that (γ,n) coincidence counting is an imperative method to detect fission events with an RPM.

Acknowledgements

I want to give my wholehearted gratitude to Dr. Débora Trombetta, for her invaluable help and guidance during this study. It would not have been possible without her. I also want to extend my thanks to Jana Petrović and Solveig Englund who have worked closely with me during this study. I want to thank everyone who took their time to read my report and give me invaluable feedback. Max Kenning also deserves a special thanks for the organising, and his wonderful wind downs during the most strenuous process of writing. Furthermore, I could not have done this study without Rays – for excellence and their collaborative partners. A distinctive thanks goes out to Kjell och Märta Beijers Stiftelse and AstraZeneca.

Contents

1 Introduction

Nuclear physics describes radioactivity, which is the mechanism behind why some nuclei spontaneously decay, yielding photons and neutrons in the form of radiation. This can be beneficial in certain circumstances, for example in the generation of electrical energy. Furthermore, the energetic state of some atoms can be utilised to create munition. Radiation is also highly lethal and can destroy DNA which can have long term effects. [1]

The smuggling and proliferation of nuclear materials is of imperative nature due to the extreme consequences the malicious use of such materials can have [2]. Hence, when using nuclear materials, systems of control must be in place, including: nuclear safety, security, and safeguards. Nuclear safety regards preventing nuclear accidents, mainly in energy production; nuclear security regards halting malicious use of nuclear material; nuclear safeguards regards stopping the spread of nuclear weapons. [3]

An example of one control system are Radiation Portal Monitors (RPMs), which function as a detector for radioactivity, measuring the radiation of objects passing through it. RPMs are excellent for combating smuggling of nuclear material, for example weapons-grade plutonium, through airports, harbors, or into large public events. Weapons-grade plutonium (WGPu) refers to plutonium with an isotopic composition of 93% ^{239}Pu, 0.65% ^{241}Pu, and 6.35% ^{240}Pu. This is however only the case for newly purified WGPu, and this composition will change due to its reactive nature [4]. This study explores and discusses detection with RPMs as a part of nuclear security and safeguards. [3]

The aim of the study was to determine the effect of shielding on the possibility of detecting nuclear material. This was tested using a simulated environment based on the Monte Carlo method.

N.B. This paper uses nuclear shorthand notation of the form A(b,c)D for reaction and (b,c) for coincidences, where A and D are heavy particles, and b and c are light particles. The A(b,c)D notation is equivalent to $\mathrm{A} + \mathrm{b} \longrightarrow \mathrm{D} + \mathrm{c}$. Notation for light particles are: n for neutron, γ for photon, and p for proton.

1.1 Photon-Matter Interaction

Photons can interact with matter through several interaction types. The type of interaction that will occur depends on the energy level of the photon and the atomic number of the absorber atom. The most common interaction types are called photoelectric effect for low-energy photons, Compton scattering for mid-energy photons, and pair production for high-energy photons. All of these interactions are detectable and are therefore important in RPMs. Fig. 1 shows the relative magnitude of the different types of interactions as a function of photon energy and the atomic number of the absorber atom. The attenuation of the photon when moving through a medium has a result dependant on all these types of interactions. [5]

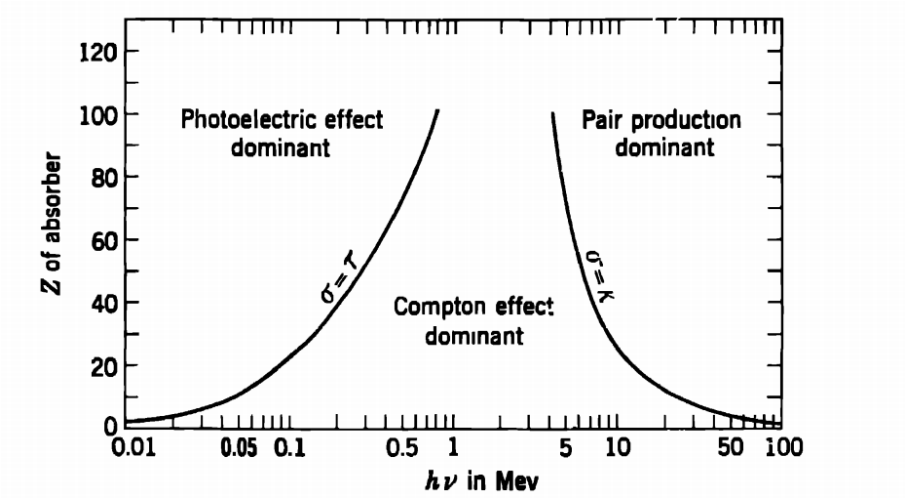

Figure 1: The relative magnitude of the different types of photon-matter interactions. The figures show what type of interaction is most prominent as a function of the energy level of the photon, as well as the atomic number of the absorber atom. Figure from [6].

1.1.1 Photoelectric Effect

An interaction between a low-energy photon and an absorber atom may lead to photoelectric effect. During this interaction the photon will be absorbed by an electron. This effect is generally the most common photon-matter interaction for photons below 1 MeV of energy. The photoelectric effect is also more frequently occurring with an absorber atom with a high atomic number, since more electrons are available to absorb the photon. [5]

1.1.2 Compton Scattering

Compton scattering is a type of interaction that may occur between a photon and an absorber atom, during which a collision deflects the photon and some of the photons energy is transferred to an electron. The amount of energy that is transferred from the photon to the electron increases with the deflection angle. A greater deflection angle correlates to a greater proportion of the energy being transferred from the photon to the electron. However, even for large angles, the photon will retain energy. Compton scattering is generally the most prominent photon-matter interaction for photon energies between 1 MeV and 5 MeV, and it is also common at other energy levels. The probability for Compton scattering increases with the number of available electrons. [5]

1.1.3 Pair Production

For photons with a total energy of more than twice that of the rest-mass of an electron, there is a possibility of pair production. The correlation between energy and mass is explained by Einstein's $E = mc^2$. Pair production is when the photon gets converted into an electron-positron pair, after interacting with an atom. Although the energy only needs to be $2m_e$ (1 MeV) for the theoretical possibility of pair production, realistically it needs to be significantly higher for it to be probable. This entails that pair production is generally only observed with high-energy photons, and it is generally the most prominent interaction for photons with energy levels above 5 MeV. [5]

1.1.4 Attenuation

The probability of any photon matter interaction occurring can be calculated by summing the probabilities per unit length for each of the aforementioned interactions occurring, see Eq. (1).

$$\mu = \tau + \sigma + \kappa \tag{1}$$

Where μ is the linear attenuation coefficient, which is the probability of any interaction occurring per unit length, and, τ, σ, and κ are the probabilities per unit length of photoelectric absorption, Compton scattering, and pair production respectively. The following relationship, seen in Eq. (2), of radiation passing through the medium may then be obtained.

$$\frac{I}{I_0} = \mathrm{e}^{-\mu t} \tag{2}$$

In this relation, I_0 is the initial intensity, and I is the intensity after passing through a thickness t of a material. [5]

1.2 Neutron-Matter Interaction

Since neutrons carry no electric charge, they are not affected by the electromagnetic force of a Coulomb field, and hence, neutron-matter interaction is only observed by collision with the nuclei of the absorbing material. There are different types of neutron-matter interaction, which can be divided into two categories, neutron scattering and neutron absorption. Neutrons with a higher kinetic energy have a lower chance of being absorbed or scattered. The thermalising of neutrons, that is slowing them down, is therefore important for an effective detection. This is due to the probability of neutrons interacting with matter being higher at low velocities. Neutron detection is important for nuclear security and safeguards due to the fact that they constitute a large part of fission products, and are therefore a good indicator of fission being present. [7]

1.2.1 Cross Section

The nuclear cross section is the probability, expressed as an area, which a neutron with a specified energy has to interact with an atom. However, in radiation detection and shielding, the macroscopic cross section is of greater interest, as it describes the probability of an interaction per unit length, Σ, which is defined by the equation, $\Sigma = N\sigma$, where N is the amount of atoms by unit volume, and σ is the nuclear cross section. Then, by summing

the macroscopic cross section for each type of interaction the total macroscopic cross section, Σ_{tot}, can be derived. The reduction in neutron intensity may then be described by Eq. (3).

$$\frac{I}{I_0} = \mathrm{e}^{-\Sigma_{\text{tot}} t} \tag{3}$$

In which I_0 and I represents the neutron intensity, before and after passing through a medium with a thickness t respectively. [5]

1.3 Neutron Multiplicity Counting

Neutron multiplicity counting (NMC) is the summation of detected neutrons, used to determine the number of neutrons being created in a certain environment during a given time. An external source is then indicated by higher-than-background levels of radiation. There are mainly two types of NMC, scatter-based (S-NMC) and capture-based (C-NMC). Today, the most commonly used type is ^{3}He-based C-NMC, which employs a ^{3}He(n,p)^{3}H reaction [5]. However, due to risk of ^{3}He shortages, S-NMC has an imperative role in radioactive detection and is the subject of much current research [3]. [7]

Unlike C-NMC, S-NMC is based mainly on elastic scattering of neutrons with light nuclei. The maximum kinetic energy of a recoil nuclei is based on the mass of said nuclei, in which a lower mass allow for more energy transfer, thus thermalising the neutron more effectively, as is described by Eq. (4).

$$E_{\text{R}} = \frac{4A}{(1+A)^2} E_{\text{n}} \tag{4}$$

Where E_{R} is the kinetic energy transferred to the recoil nuclei, A is the atomic mass number of the nuclei, and E_{n} is the kinetic energy of the incident neutron. [5]

1.4 Coincidences

A coincidence is the detection of two particles close in time to one another, and in the realm of this study, from the same fission event. To know whether or not the particles originate from the same fission event, a method of timed gates is employed, which sets a time window of a few nanoseconds after the detection of the first particle. However, this will experimentally not be 100% accurate. This is used to acquire a more accurate detection of fission; a fission event creates both photons and neutrons. The detection of these particles in coincidence will give an assertive correlation to a fission event, and further a fissile material.

The time differences are defined between the detection of one particle in one detector, and the following detection of another particle in another detector. Two of the primary types of coincidences are neutron-neutron, (n,n), and photon-neutron, (γ,n). The time difference in (γ,n) coincidences is expected to be larger than in (n,n) coincidences when the particles originate from the same fission event, due to the significant difference in mass and coincidental velocities between photons and neutrons. [3]

1.5 Scintillator Detectors

Scintillator detectors are based on a scintillator material which emits light when hit by radiation, and can be used as a detector in RPM systems. This light is then captured and measured by photomultiplier tubes and photodetectors. These types of detectors, particularly those based on organic scintillators, inhabit a very fast response time. With the help of Pulse Shape Discrimination, which is further explained in 1.5.1, can these detectors also distinguish between photon and neutron radiation. [5]

Liquid scintillators are solutions with a dissolved organic scintillator. An advantage of liquid scintillators is that they have a good scalability and have the possibility to vary much in size, providing a great versatility in practical applications. [5]

EJ-309 is the liquid scintillator used in the KTH RPM prototype [2]. This scintillator

is specifically good for Pulse Shape Discrimination, between photons and neutrons. It also has a refractive index which is very close to that of the photomultiplier tubes, which lowers the possibility of light being deflected when leaving the scintillator and entering the photomultiplier tube; giving a more accurate reading. [8]

1.5.1 Pulse Shape Discrimination

To be able to differentiate between photons and neutrons in a scintillator detector, Pulse Shape Discrimination (PSD) is used. PSD functions by analysing the current pulses generated by the photodetection. Different levels of radiation cause different scintillation light signals, which in turn cause different electrical signals. The difference in scintillation light also depends on the scintillator material used, and their light decay time. This means that different scintillator materials have different possibilities to discriminate against different types of radiation. [9]

1.6 Monte Carlo N-Particle

Monte Carlo N-Particle (MCNP) is a simulation program developed at Los Alamos National Laboratory, which is based on the Monte Carlo simulation method which is in this experiment used to simulate radioactivity, and detection. This is done by simulating N histories, which can be seen as smaller simulations following a particle and its products, in a three-dimensional environment. The environment is made up of cells, which function as 3D bodies made of different materials, and therefore inhabit different characteristics. Interactions between particles are then calculated and the different events are recorded. For example, one history could start with a fast neutron that induces fission in a nucleus which creates new neutrons and photons, all of which can follow the same pattern, with inducing a fission and creating new particles. When all particles are outside the determined 3D space, the history has finished, and all the data noted. The Monte Carlo method itself utilises a probability distribution and multiple simulations to get a numerically accurate value for a system that is unpredictable and random. Because of this, it

yields a lower and upper bound to approximate the real output, instead of calculating for a specific value. [10]

1.7 Radiation Portal Monitors

RPMs are devices used to detect radioactive decay, especially fission, both induced and spontaneous, and if detected, will sound an alarm. RPMs measure the radioactive levels when an object, such as a person, a car or a boat, passes through a portal. The most common detection method is with ^{3}He proportional detectors, as described in section 1.3, but it can also be done with scintillator detectors, such as with EJ-309 [5]. [2]

RPM detectors work on the principle of detecting radiation by it interacting with some medium which reacts when hit by radiation, for example the scintillator material, which emits light as a result of interacting with radiation. It is therefore of importance to detect all types av photon-matter interactions, as well as maximising the nuclear cross section for neutron-matter interaction. [2]

The prototype that is being constructed at KTH will have the ability to pinpoint from where the radiation is coming from. When a nuclear material decays through fission both neutrons and photons are emitted, and because of the longer travel time of neutrons due to their larger mass there will be a time difference for the detection of the particles from the same fission event. [5]. This enables the possibility to measure the relative time of flight for the particles, which can be used to create a probability function of where the source is located. [2]

2 Method

Simulations were conducted and data regarding the shielding of radiation originating from a WGPu source was gathered with the help of MCNP. The data was then processed and plotted.

2.1 MCNP Simulations

Surfaces were defined and the interior hull of these surfaces were defined as different cells. Compositions of the different materials of the cells were determined, with a source consisting of 93.6% ^{239}Pu and 6% ^{240}Pu, and a scintillator consisting of 48% ^{1}H and 52% ^{12}C, see App. A. In the simulated environment the WGPu source with a mass of 190g was located in the middle of a cylindrical shell. This cylindrical shell functioned as the shield of polystyrene and lead, respectively per simulation. Around the source, two sets of four EJ-309 scintillator detectors were placed, all with a diameter of 12.7 cm. The distance between the detectors and the source was 50 cm. The geometric environment is shown in Fig. 2.

In total seven simulations were run, three control simulations with 10^6 histories and a bare source. Two with 2×10^5 histories and polystyrene shielding, both with 1.0 cm and 3.0 cm of thickness. And two with 2×10^5 histories and lead shielding, with the same thickness levels as polystyrene.

A particle is counted as detected if it is scattered inside the detector cell, that is when the kinetic energy of the particle is transferred to the scintillator. In a real-world experiment, a portion of this energy would be released as scintillation light and detected by the photodetector. The yielded data from the program contained the position, energy, and time of the particle.

2.2 Data Analysis

The data output from the MCNP simulations was processed by analysing the particles that were counted as detected and noting their information on energy, time, and position, while particles that did not scatter in the detectors were omitted from the data along with their respective information. This created new lists of (γ,n) and (n,n) coincidences, and of single neutrons.

The data acquired was then plotted with the aim of detecting discrepancies in coin-

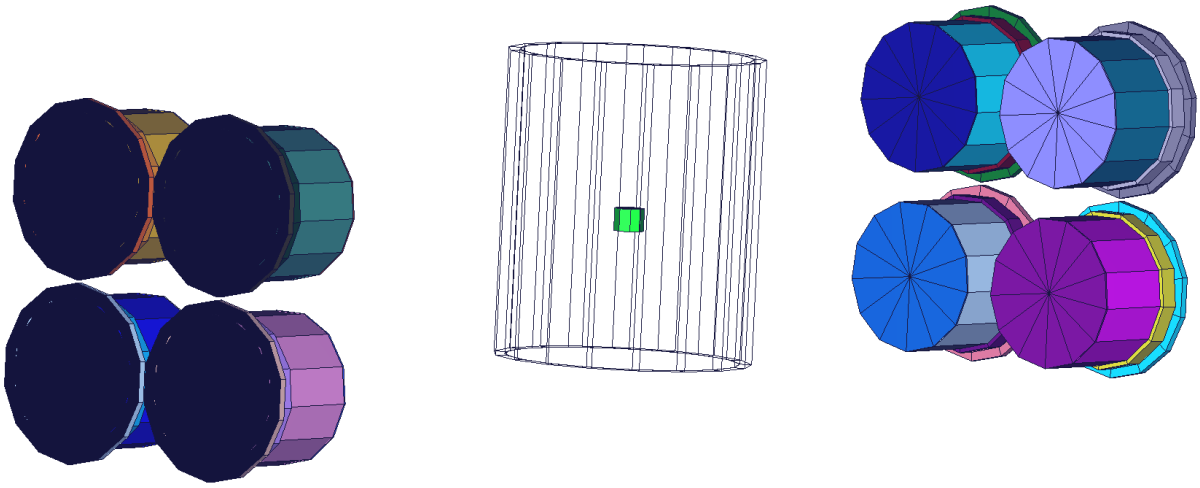

Figure 2: The geometry of the simulations. The small cylinder in the centre is the plutonium source, the wire-framed cylinder is the shield, and the outer cylinders are the scintillator detectors

cidence time difference, energy levels, and the count rate. The data with shielding was contrasted to the control simulations.

3 Results

The data is presented as control data with the time difference between (γ,n) and (n,n) as well as the energy of (γ,n). The count rate data is also presented, contrasted with the control data. There are several graphs in App. B.

3.1 Control

Fig. 3 shows the total number of counts for the time difference and energy of the control simulations with regards to (γ,n) and (n,n). The energy of detected neutrons is higher than the energy of the detected photons in (γ,n). The number of counts is also higher towards the low-end of the energy-spectrum. The average time difference between neutrons in (n,n) is lower than the average time difference between photons and neutrons in (γ,n).

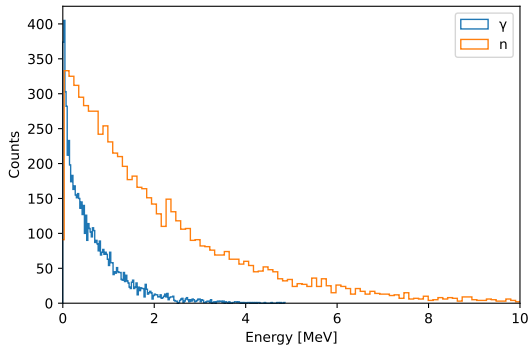

(a) Energy of γ and neutrons in (γ,n) coincidence.

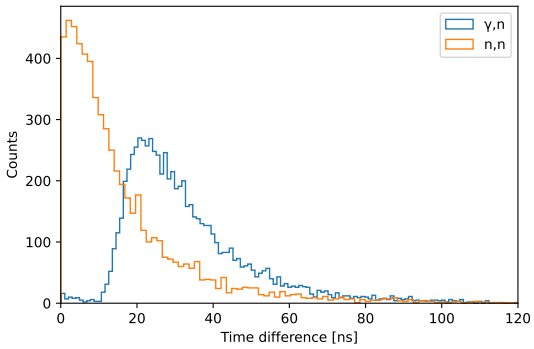

(b) Coincidence time difference for (γ,n) and (n,n).

Figure 3: Data from the control simulations. The simulations had a total 3×10^6 histories.

3.2 Count Rate

Fig. 4 and 5 shows the effect that the different types of shielding had on the count rate and time difference with regards to (γ,n) and (n,n). Fig. 6 and Tab. 1 shows how the total count rate is affected by the radiation shielding with regards to (γ,n), (n,n) and single neutrons. The mean value of the time difference have not considerably changed when adding shielding. For the detection of (γ,n) the 3.0 cm shields affected as such; lead shielded 71.61% and polystyrene shielded 61.53% of the radiation. For the detection of (n,n) the 3.0 cm shields affected as such; lead shielded 14.79% and polystyrene shielded 77.91% of the radiation.

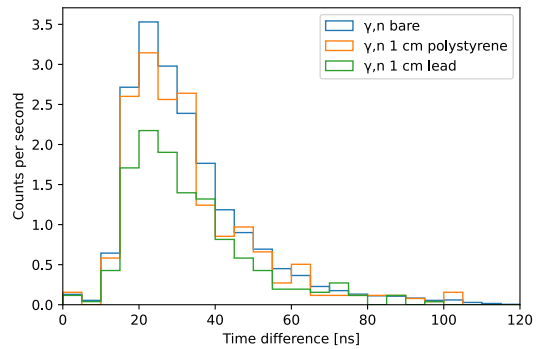

(a) Time difference for (γ,n), normalised by count rate, and with 1 cm of shielding

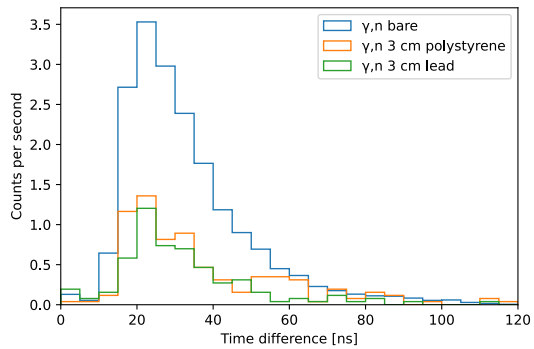

(b) Time difference for (γ,n), normalised by count rate, and with 3 cm of shielding

Figure 4: Time difference for (γ,n), normalised by count rate, and with shielding

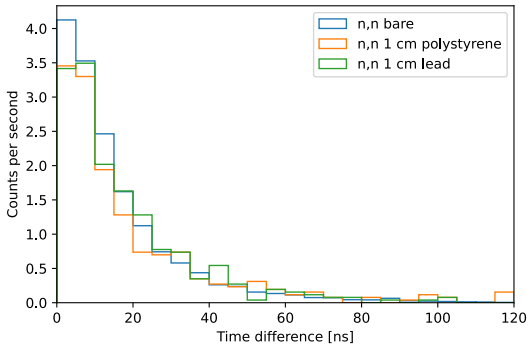

(a) Time difference for (n,n), normalised by count rate, and with 1 cm of shielding

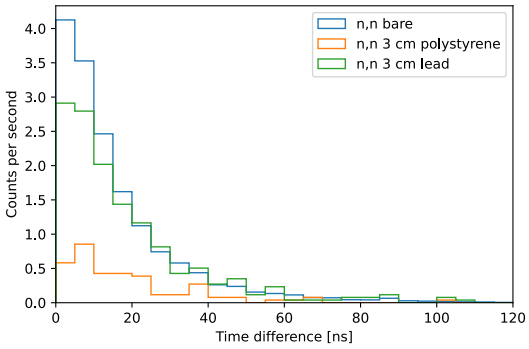

(b) Time difference for (n,n), normalised by count rate, and with 3 cm of shielding

Figure 5: Time difference for (n,n), normalised by count rate, and with shielding

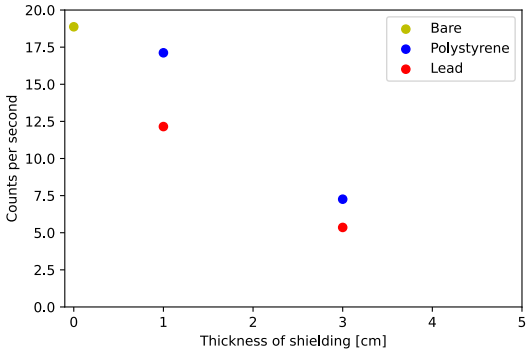

(a) Count rate for (γ,n) coincidence, and different shielding

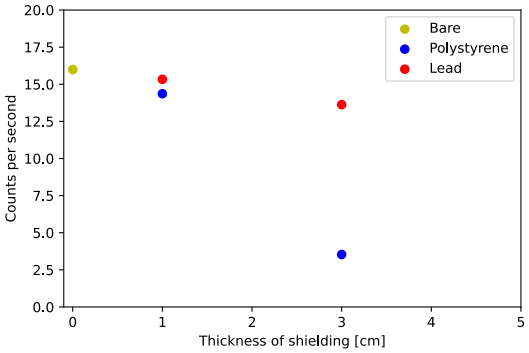

(b) Count rate for (n,n) coincidence, and different shielding

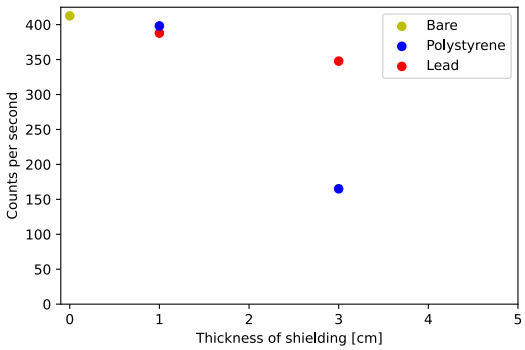

(c) Count rate for single neutrons, and different shielding

Figure 6: Count rate for the different simulations

Table 1: Count rate data

Detection type	**Material**	**Thickness [cm]**	**Count rate [s^{-1}]**	**Shielding**
(γ,n)	None	N/A	18.87	0%
(γ,n)	Polystyrene	1.0	17.12	9.28%
(γ,n)	Polystyrene	3.0	7.259	61.53%
(γ,n)	Lead	1.0	12.15	35.61%
(γ,n)	Lead	3.0	5.357	71.61%
(n,n)	None	N/A	15.99	0%
(n,n)	Polystyrene	1.0	14.36	10.18%
(n,n)	Polystyrene	3.0	3.533	77.91%
(n,n)	Lead	1.0	15.33	4.02%
(n,n)	Lead	3.0	13.63	14.79%
n	None	N/A	412.6	0%
n	Polystyrene	1.0	398.1	3.495%
n	Polystyrene	3.0	165.1	59.99%
n	Lead	1.0	387.9	5.979%
n	Lead	3.0	347.8	15.69%

4 Discussion

It is possible to discern the prominence of the different types of photon interaction using the energy spectrum. The count rate data also gives a good understanding of how the different types of shielding affect the detection. There are also some improvements worth to explore for the RPM. The statistical uncertainty for the shielded simulations is higher than the control, since the simulations are smaller. Thus, indicating a clear improvement for further studies.

4.1 Prominence of Interactions

The energy of the detected photons, as seen in Fig. 3a, show that the main type of interaction that occurs between photons and the detector is Compton scattering, but photoelectric effect is prevalent as well. Some pair production can also occur although such interaction was barely detected and is unlikely. This is logical as the detectors are composed of carbon and hydrogen, see App. A; elements known for their low atomic numbers. This is apparent when combining these assumptions with Fig. 7, which shows that the energy detected, lower than 2 MeV, and the atomic numbers of the absorber atoms, lower than 12, is in the area with Compton scattering and photoelectric effect.

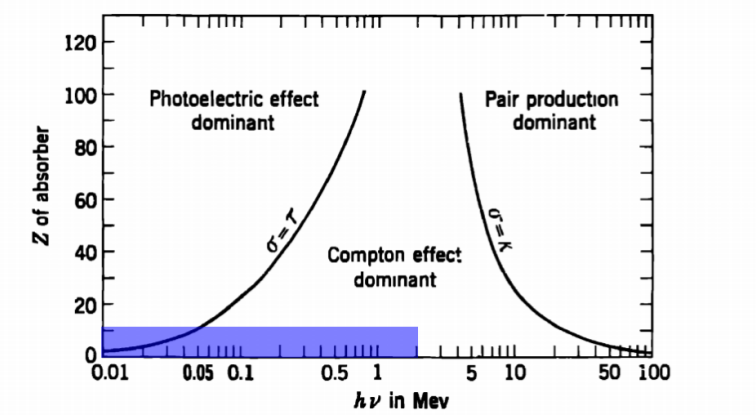

Figure 7: The area of where the interactions take place

If pair production was the most prominent type of interaction, there would be a much

greater number of counts in the high-energy region. Likewise, if photoelectric effect was the most prominent, a larger spike should be seen in the very low-energy region, and a faster drop-off. However, the photoelectric effect still seems to be delectable.

To enable the detection of high energy photons, the composition of the detector, that is the scintillator material, would allow for better results with a higher atomic number. This is due to the fact that a higher atomic number of the absorber atom will increase the relative magnitude of pair production at lower energies, see Fig. 1 [5].

Different scintillator fluids should not affect the result particularly, due to all organic scintillators being composed of mainly hydrogen and carbon, which both have low atomic numbers. Because of this, the interaction between photons and organic scintillators will only be able to detect pair production if the photon have very high energy. To enable the detection of pair production in RPMs, it would instead be an idea to let the interaction occur in the shell outside the liquid and detect the created electron or positron, by utilising a material with a high atomic number for the shell. This could be a subject of further research to enable better detection of RPMs.

4.2 Count Rate

The count rate went down with added shielding, and the data also show a clear difference between how shielding affect (n,n) and (γ,n) coincidences. Because of the low atomic numbers of the isotopes in the composition of polystyrene, the shielding was more effective against neutrons than photons. This is seen in polystyrene shielding 10% and 78% for 1.0 cm and 3.0 cm respectively for (n,n), while the corresponding numbers for (γ,n) are 10% and 62%. A thicker shielding of polystyrene will therefore have a greater impact on the count rate for (n,n) than for (γ,n) coincidences.

The opposite can be said for lead shielding. 3.0 cm of lead shielding, shielded 15% of (n,n) and 72% of (γ,n). While lead shields better for (γ,n) than polystyrene, its shielding capability for (n,n) is very limited, while polystyrene is good at shielding both types of coincidences.

Regarding the detecting method; (γ,n) coincidence may be used with a higher degree of certainty than (n,n). This is because the count rate for (γ,n) is higher than (n,n) at their lowest levels. Hence, if the shielding material is unknown, (γ,n) will have a better chance of having a count rate higher than the threshold of detection for the RPM; the RPM will sound the alarm the same if the count rate is twice the threshold as just above it. The application of radioactive shielding in the realm of RPMs is smuggling, and the shielding material will therefore rarely be known.

As for the detection of single neutrons; the lead shield barely absorbs any radiation, while the polystyrene makes a considerable impact. Again pressing on the fact of using a detection method that includes photons, due to them not being affected by polystyrene as much as neutrons, although they are more susceptible to being stopped by lead.

However, it should be mentioned that there are several other shielding materials and these could also be categorised as high atomic number, and low atomic number, as well as density. In this study, a high density, high atomic number material has been tested in the form of lead, as well as a low density, low atomic number material in the form of polystyrene. A higher density should always lead to better shielding due to there being more atoms available for interaction. The atomic number, on the contrary, will cause different effects for different types of radiation; a high atomic number is superior for photon-matter interaction, but inferior for neutron-matter interaction. This is a subject of further studies.

4.3 Further Studies of the RPM

The geometry of the simulated RPM could be an improvement. All the detectors are gathered at two places, in principle, only functioning as two large detectors, instead of eight small. It is not certain that this would increase the count rate or the detection efficiency of the RPM. It is however something that is worth exploring.

Currently, the shell that contains the scintillator liquid is made from aluminium, which might have an impact on the detection. If the shell is made from a material with a higher

atomic number, the possibility of pair production being detected might increase, at the same time, the count rate of photons will probably decrease and might worsen the overall detection efficiency of the RPM. The effect the shell material has on the detection can be explored.

4.4 Conclusion

The conclusion is that (γ,n) coincidence counting is an important method of detection, due to the higher chance of the count rate being above the threshold of detection, regardless of shielding. This being said, (n,n) and single neutrons should not be omitted from the methods of detection, since they will give a better count rate than (γ,n) if the shielding is only good at shielding photons. Further studies should also explore the geometry and materials of the RPM to see if the detection can be extended to include pair production, as well as increasing the overall count rate.

References

[1] Cottingham WN, Greenwood DA, Greenwood DA. An introduction to nuclear physics. Cambridge University Press; 2001.

[2] Petrović J, Göök A, Cederwall B. Rapid imaging of special nuclear materials for nuclear nonproliferation and terrorism prevention. Science Advances. 2021;7(21).

[3] Trombetta DM, Klintefjord M, Axell K, Cederwall B. Fast neutron-and γ-ray coincidence detection for nuclear security and safeguards applications. Nuclear Instruments and Methods in Physics Research Section A: Accelerators, Spectrometers, Detectors and Associated Equipment. 2019;927:119–124.

[4] Keegan RP, Gehrke RJ. A method to determine the time since last purification of weapons grade plutonium. Applied Radiation and Isotopes. 2003;59(2-3):137–143.

[5] Knoll GF. Radiation Detection and Measurement. Wiley; 2000.

[6] Evans RD. The atomic nucleus. vol. 582. McGraw-Hill New York; 1955.

[7] Rinard P. Neutron interactions with matter. Passive nondestructive assay of nuclear materials. 1991;(375-377).

[8] NEUTRON/GAMMA PSD EJ-301, EJ-309. Eljen Technology; 2018.

[9] Roush ML, Wilson MA, Hornyak WF. Pulse shape discrimination. Nuclear Instruments and Methods. 1964;31(1):112–124.

[10] X-5 Monte Carlo Team. MCNP — A General Monte Carlo N-Particle Transport Code, Version 5 Volume I: Overview and Theory; 2008.

[11] McConn RJ, Gesh CJ, Pagh RT, Rucker RA, Williams III R. Compendium of material composition data for radiation transport modeling. Pacific Northwest National Lab.(PNNL), Richland, WA (United States); 2011.

A Composition of Materials

Table 2: Tables of composition [11]

(a) Composition of WGPu

Isotope	Proportion
^{238}Pu	0.01%
^{239}Pu	93.6296%
^{240}Pu	5.991%
^{241}Pu	0.1997%
^{242}Pu	0.03%
^{241}Am	0.1398%

(b) Composition of air inside detectors

Isotope	Proportion
^{14}N	75.5636%
^{16}O	23.1475%
^{40}Ar	1.2838%
^{36}Ar	0.0043%
^{38}Ar	0.0008%

(c) Composition of EJ-309

Isotope	Proportion
^{1}H	48%
^{12}C	52%

(d) Composition of polystyrene

Isotope	Proportion
^{1}H	7.7421%
^{12}C	92.2579%

(e) Composition of air

Isotope	Proportion
^{12}C	0.0124%
^{14}N	75.5268%
^{16}O	23.1781%
^{40}Ar	1.2827%

(f) Composition of aluminium

Isotope	Proportion
^{27}Al	100%

(g) Composition of Lead

Isotope	Proportion
Pb	100%

B Graphs

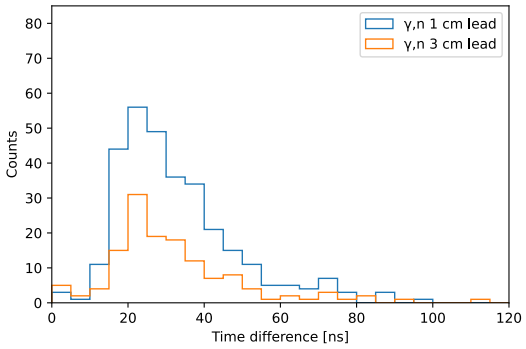

(a) Time difference for (γ,n) with lead shielding

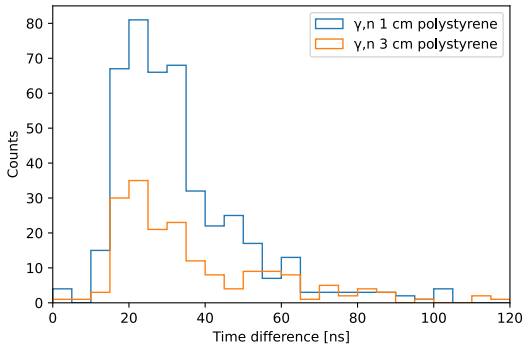

(b) Time difference for (γ,n) with polystyrene shielding

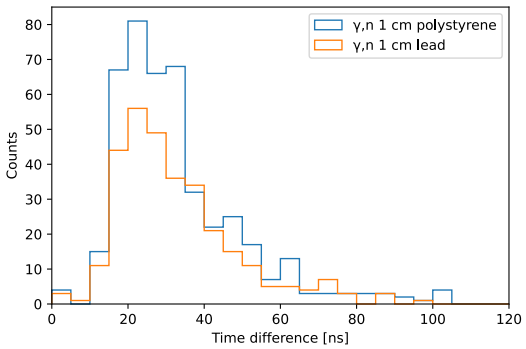

(c) Time difference for (γ,n) with 1 cm of shielding

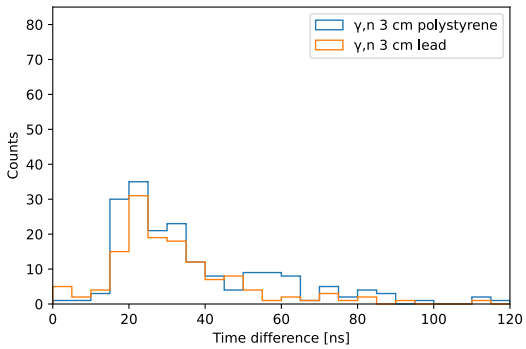

(d) Time difference for (γ,n) with 3 cm of shielding

Figure 8: Time difference for (γ,n) with different shielding materials, and thickness

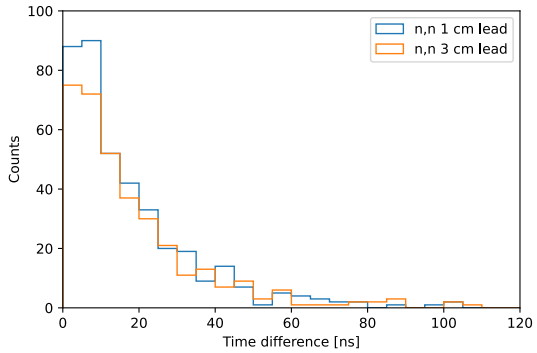

(a) Time difference for (n,n) with lead shielding

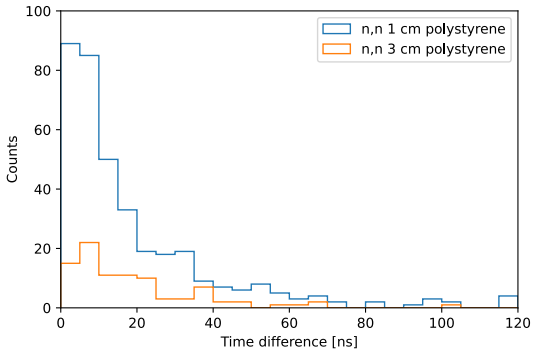

(b) Time difference for (n,n) with polystyrene shielding

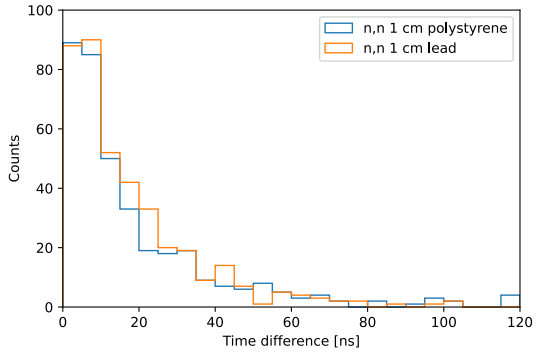

(c) Time difference for (n,n) with 1 cm of shielding

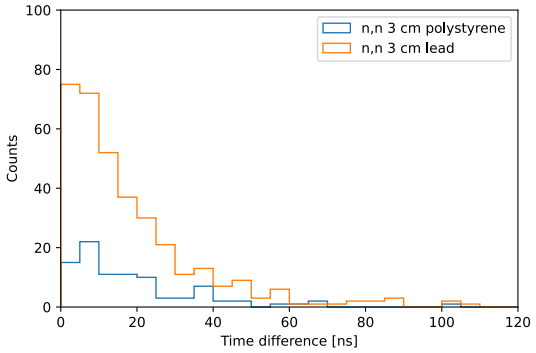

(d) Time difference for (n,n) with 3 cm of shielding

Figure 9: Time difference for (n,n) with different shielding materials, and thickness

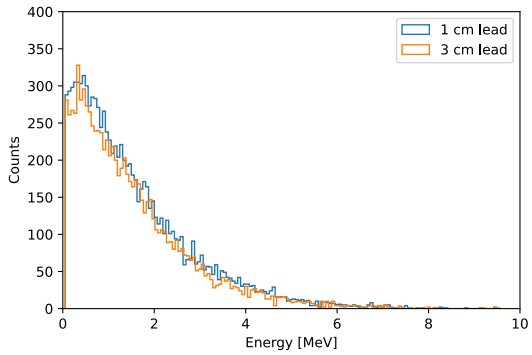

(a) Energy for single neutrons with lead shielding

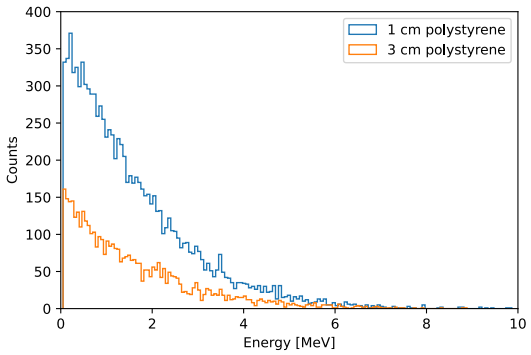

(b) Energy for single neutrons with polystyrene shielding

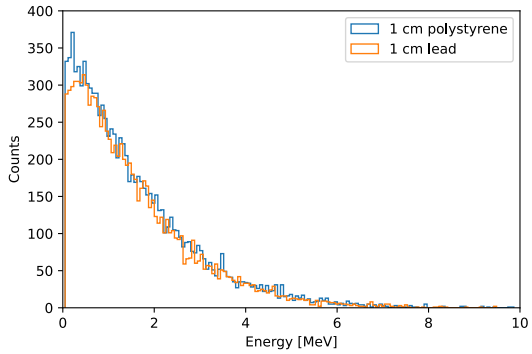

(c) Energy for single neutrons with 1 cm of shielding

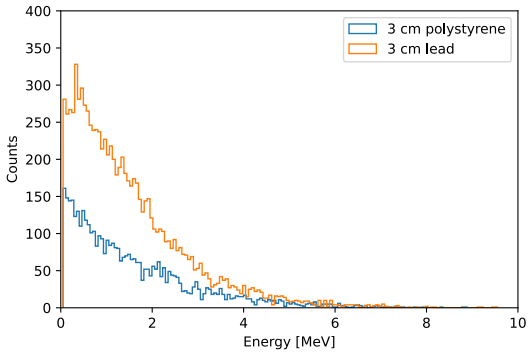

(d) Energy for single neutrons with 3cm shielding

Figure 10: Energy for single neutrons with different shielding materials, and thickness

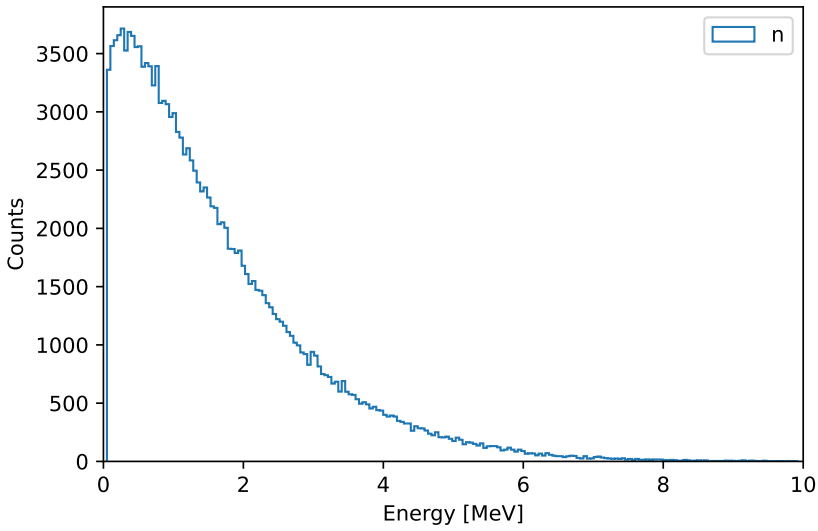

Figure 11: Energy of single neutrons. The simulations had a total 3×10^6 histories.